Transition-metal complexes of cyclopentadienylphosphines
XIV. Reduction reactions of various derivatives of the chelate fragment $[\{\eta^5:\eta^1\text{-}C_5H_4(CH_2)_2PPh_2\}M^{III}]^{2+}$, M = Rh, Ir

Inja Lee, Françoise Dahan, André Maisonnat [*], René Poilblanc

*Laboratoire de Chimie de Coordination du CNRS, UPR 8241, lié par conventions à l'Université Paul Sabatier et à l'Institut National
Polytechnique, 205 route de Narbonne, 31077 Toulouse Cedex, France*

Received 16 July 1996; revised 19 September 1996

Abstract

Iodide abstraction by silver salts from the complexes $[\{\eta^5:\eta^1\text{-}C_5H_4(CH_2)_2PPh_2\}MI_2]$, (1, M = Rh; 2, M = Ir), yields products whose structures are dependent on the coordinating ability of the anion originally associated with silver. Silver trifluoroacetate gave fully characterized disubstituted derivatives of the type $[\{\eta^5:\eta^1\text{-}C_5H_4(CH_2)_2PPh_2\}M(CF_3COO)_2]$, (3, M = Rh; 4, M = Ir), in which the trifluoroacetate anions are bound in a monodentate fashion. Silver hexafluorophosphate gave a dinuclear dicationic compound $[\{(\eta^5:\eta^1\text{-}C_5H_4(CH_2)_2PPh_2)Rh(\mu\text{-}I)\}_2][PF_6]_2$, 5, in which the metal atoms are bridged by iodide. Complex 3 crystallizes in the triclinic space group $P\bar{1}$ with two molecules in the unit cell, with $a = 8.3060(7)$ Å, $b = 18.289(2)$ Å, $c = 7.9724(8)$ Å, $\alpha = 94.178(8)°$, $\beta = 106.477(8)°$, $\gamma = 93.964(7)°$ and $V = 1153.2(2)$ Å³. Least squares refinement leads to conventional R values $R(F_o) = 0.041$ and $Rw = 0.042$ for 3361 reflections having $I > 3\sigma(I)$. Complex 5 crystallizes in the monoclinic space group $P2_1/c$ with two molecules of 5 and two molecules of acetone in the unit cell, the dimensions of which are $a = 13.838(1)$ Å, $b = 13.403(1)$ Å, $c = 14.362(1)$ Å, $\beta = 104.73(1)°$ and $V = 2576.2(5)$ Å³. Least squares refinement leads to conventional R values $R(F_o) = 0.034$ and $Rw = 0.040$ for 2246 reflections having $I > 2\sigma(I)$. Surprisingly, the treatment of the bis-trifluoroacetato complexes 3 and 4 with lithium triethylhydroborate yields quantitatively the ethylene metal(I) derivatives $[\{\eta^5:\eta^1\text{-}C_5H_4(CH_2)_2PPh_2\}M(C_2H_4)]$, (9, M = Rh; 10, M = Ir), whereas unstable polyhydride derivatives result from the reaction of the diiodo complex 1 with lithium triethylhydroborate, and from the reaction of the bis-trifluoroacetato complex 3 with sodium tetrahydroborate. The chemical or electrochemical reduction of complex 5 leads to the solvated rhodium(III) species, $[\{\eta^5:\eta^1\text{-}C_5H_4(CH_2)_2PPh_2\}Rh(THF)][PF_6]$, 6, together with a dinuclear rhodium(II) species, $[\{\eta^5:\eta^1\text{-}C_5H_4(CH_2)_2PPh_2\}RhI\}_2]$, 7. The protonation of 7 with tetrafluoroboric acid affords the monocationic dinuclear complex $[\{\eta^5:\eta^1\text{-}C_5H_4(CH_2)_2PPh_2\}RhI\}_2H][BF_4]$, 8, in which the added proton bridges the rhodium atoms.

Keywords: Reduction; Heterodifunctional ligand; Chiral

1. Introduction

The reasons for interest in substituted cyclopentadienyl metal compounds [1] are demonstrated by their ability to act as catalysts in numerous processes (hydrogenation and asymmetric hydrogenation [2], cross-coupling reactions [3], Ziegler–Natta polymerization [4]) as well as material precursors (see for example Ref. [5]). Cyclopentadienyl ligands bearing a functionalized side chain were designed and used to synthesize new mono

or dimetal complexes. For example, we and others, have used cyclopentadienyldiphenylphosphine [6], in which the Cp and PPh₂ functions are directly linked, to yield homo- [7,8] and hetero- [9] dimetallic species in which the heterodifunctional ligands act as a bridging unit of the metal centers. In contrast, the introduction of a 'spacer group' between the two functions allows the formation of a chelated fragment whose stability relative to the parent cyclopentadienyl compounds containing tertiary phosphines is possibly increased. Numerous papers have dealt with the preparation of chelate complexes using modified Cp ligands in which the additional functionality — phosphine [7,10–13], diphosphine and diarsine [13], amine [4,14–21], amide [22],

[*] Corresponding author. Fax: (+33) 5 61 55 30 03; e-mail: maisonat@lcc-toulouse.fr.

imide [23], alkoxide [24], or alkenyl [25] — is separated from the cyclopentadienyl or tetramethylcyclopentadienyl group by an alkyl or alkylsilyl chain.

Recently, we reported the synthesis and structural properties of new chelated metal(I) and metal(III) rhodium and iridium complexes with (cyclopentadienylethyl)diphenylphosphine [26]. Among these complexes, the diiodo species $[\{\eta5:\eta1\text{-}C_5H_4(CH_2)_2PPh_2\}MI_2]$, (**1**, M = Rh; **2**, M = Ir), appeared as suitable precursors for the synthesis, by halide abstraction, of derivatives in which the cationic fragment $[\{\eta^5:\eta^1\text{-}C_5H_4(CH_2)_2PPh_2\}M]^{2+}$ forms monometallic or bimetallic bridged complexes depending on the nature of the anionic ligand. We report now the behavior of these derivatives towards hydrides and in electrochemical experiments.

2. Experimental section

2.1. General remarks

All reactions and manipulations were routinely performed under dinitrogen or argon in Schlenk-type glassware. All solvents were appropriately purified before use by distillation from sodium–benzophenone or CaH$_2$.

Microanalyses were performed by the 'Service de Microanalyse' du Laboratoire de Chimie de Coordination. DCI and/or EI mass spectra were recorded on a Nermag R10-10 instrument. ^{1}H NMR spectra were obtained at 200.13 MHz on Bruker AC 200 FT, or at 250.1 MHz on Bruker AM 250 FT spectrometers. ^{31}P NMR spectra were recorded at 32.4 MHz on Bruker AC 80 FT, at 81.01 MHz on Bruker AC 200 FT, or at 101.22 MHz on Bruker AM 250 FT spectrometers. Chemical shifts were referenced to external H$_3$PO$_4$.

2.2. Preparation of compounds

The starting materials $[\{\eta^5:\eta^1\text{-}C_5H_4(CH_2)_2PPh_2\}RhI_2]$, **1**, and $[\{\eta^5:\eta^1\text{-}C_5H_4(CH_2)_2PPh_2\}IrI_2]$, **2**, were prepared according to published procedures [26].

2.2.1. $[\{\eta^5:\eta^1\text{-}C_5H_4(CH_2)_2PPh_2\}Rh(CF_3COO)_2]$, 3

To a white suspension of silver trifluoroacetate (92 mg, 0.42 mmol) in dichloromethane (5 ml) was added at room temperature a red-brown solution of **1** (135 mg, 0.21 mmol) in dichloromethane (5 ml). The color of the solution turned quickly from red-brown to orange. After 30 min stirring, the solution was filtered and the volume reduced under vacuum to 5 ml. Pentane (1 ml) was then added to precipitate **3** as an orange solid (102 mg; 0.16 mmol; 76%). Anal. Calcd. for $C_{23}H_{18}F_6O_4PRh$: C, 45.57; H, 2.99. Found: C, 45.22; H, 3.21.

2.2.2. $[\{\eta^5:\eta^1\text{-}C_5H_4(CH_2)_2PPh_2\}Ir(CF_3COO)_2]$, 4

To a suspension of silver trifluoroacetate (74 mg; 0.33 mmol) in dichloromethane (10 ml) was added a red-brown solution of **2** (120 mg; 0.16 mmol) in dichloromethane (5 ml). The mixture was stirred for 30 min affording slowly a brown-yellow solution and a white precipitate. The solution was filtered and the solvent removed under vacuum.The residue recrystallized from toluene–pentane to give a brown-orange solid (86 mg; 0.12 mmol; 75%). Anal. Calcd. for $C_{23}H_{18}IrO_4P$: C, 39.72; H, 2.61. Found. C, 39.79; H, 2.58.

2.2.3. $[\{[\eta^5:\eta^1\text{-}C_5H_4(CH_2)_2PPh_2\}Rh(\mu\text{-}I)\}_2][PF_6]_2$, 5

To a suspension of silver hexafluorophosphate (54 mg; 0.21 mmol) in dichloromethane (15 ml) was added dropwise a red solution of **1** (126.6 mg; 0.20 mmol) in dichloromethane (5 ml). The mixture was stirred for 30 min affording a brown-yellow solution and a white precipitate. The solution was filtered and the solvent removed under vacuum to give a light brown solid (108 mg; 0.083 mmol; 83%). Anal. Calcd. for $C_{38}H_{36}F_{12}I_2P_4Rh_2$: C, 35.00; H, 2.78. Found: C, 34.66; H, 2.92.

Using similar experimental conditions the treatment of **1** with AgBF$_4$ yielded the tetrafluoroborate salt as red-brown crystals in similar yield. Anal. Calcd. for $C_{38}H_{36}B_2F_8I_2P_2Rh_2$: C, 35.39; H, 2.97. Found: C, 35.27; H, 2.94.

2.2.4. $[\{\eta^5:\eta^1\text{-}C_5H_4(CH_2)_2PPh_2\}Rh(THF)\}][PF_6]$, 6, and $[\{[\eta^5:\eta^1\text{-}C_5H_4(CH_2)_2PPh_2\}RhI]_2]$, 7

2.2.4.1. Method A: reduction of $[\{[\eta^5:\eta^1\text{-}C_5H_4(CH_2)_2PPh_2\}Rh(\mu\text{-}I)\}_2][PF_6]_2$, 5 by lithium triethylhydroborate. Two equivalents of LiBHEt$_3$ (100 ml of a 1.0 M solution in THF) were added to a solution of compound **5** (65.2 mg; 0.05 mmol) in THF (10 ml) at −78 °C and then stirred for 2 h at room temperature. The solution turned progressively from red-brown to green. The solvent was removed on a vacuum line to give a green residue. The ^{31}P{^{1}H} NMR in acetone-d_6 of this green solid indicated the presence of two different compounds (noted **6** and **7**) in almost equal quantities. On ^{31}P{^{1}H} NMR spectrum, the compound **6** exhibits a doublet centered at 65.60 ppm ($^1J_{P-Rh}$ = 179.0 Hz) and a septuplet centered at −138.80 ppm for the hexafluorophosphate anion ($^1J_{P-F}$ = 708 Hz), while the compound **7** exhibits a single doublet centered at 38.60 ppm ($^1J_{P-Rh}$ = 167.8 Hz) (Table 1). Compound **7** was first extracted from the green residue by dissolution in a toluene–pentane (50/50) mixture. Evaporation of the solvents gave an analytically pure compound **7** as a pale green solid (17.75 mg, 35% yield based on rhodium). Anal. Calcd. for $C_{38}H_{36}I_2P_2Rh_2$: C, 45.00; H, 3.58. Found: C, 45.01; H, 3.72. Mass spectra

Table 1
31P{1H} NMR data of the isolated ((cyclopentadienylethyl)diphenylphosphine)rhodium and iridium complexes

	$\delta(^{31}P)$ (ppm)	$^1J_{P-Rh}$ (Hz)
[{η^5:η^1-C$_5$H$_4$(CH$_2$)$_2$PPh$_2$}RhI$_2$], 1 [a]	54.58(d) [c]	146.7
[{η^5:η^1-C$_5$H$_4$(CH$_2$)$_2$PPh$_2$}IrI$_2$], 2 [a]	15.52(s)	
[{η^5:η^1-C$_5$H$_4$(CH$_2$)$_2$PPh$_2$}Rh(CF$_3$COO)$_2$], 3 [a]	66.57(d)	149.7
[{η^5:η^1-C$_5$H$_4$(CH$_2$)$_2$PPh$_2$}Ir(CF$_3$COO)$_2$], 4 [a]	39.40(s)	
[{(η^5:η^1-C$_5$H$_4$(CH$_2$)$_2$PPh$_2$}Rh(μ-I))$_2$][PF6]$_2$, 5 [b]	69.10(d)	142.6
[{η^5:η^1-C$_5$H$_4$(CH$_2$)$_2$PPh$_2$}Rh(C$_4$H$_8$O)][PF$_6$], 6 [b]	65.60(d)	179.0
[{(η^5:η^1-C$_5$H$_4$(CH$_2$)$_2$PPh$_2$}RhI)$_2$], 7 [b]	38.60(d)	167.8
[{(η^5:η^1-C$_5$H$_4$(CH$_2$)$_2$PPh$_2$}RhI)$_2$(μ-H)][BF$_4$], 8 [d]	31.30(d)	129.7
[{η^5:η^1-C$_5$H$_4$(CH$_2$)$_2$PPh$_2$}Rh(C$_2$H$_4$)], 9 [c]	69.39(d)	213.6
[{η^5:η^1-C$_5$H$_4$(CH$_2$)$_2$PPh$_2$}Ir(C$_2$H$_4$)], 10 [c]	26.97(s)	

[a] In CH$_2$Cl$_2$–C$_6$D$_6$.
[b] In acetone-d_6.
[c] In C$_6$D$_6$.
[d] In CD$_2$Cl$_2$.
[e] (s) for singlet, (d) for doublet.

(DCI/NH$_3$) m/e 508 for [M/2 + H$^+$] and 525 for [M/2 + NH$_4^+$]. Compound 6 was then extracted from the remaining residue with 5 ml of acetone. This led to a deep green solution from which compound 6 precipitated as a green solid after addition of 1 ml of pentane and cooling at -20°C (28.8 mg, 40% yield based on rhodium). Anal. Calcd. for C$_{23}$H$_{26}$F$_6$IOP$_2$Rh: C, 38.15; H, 3.62. Found: C, 38.28; H, 3.59.

2.2.4.2. Method B: reduction of [{(η^5:η^1-C$_5$H$_4$(CH$_2$)$_2$PPh$_2$}Rh(μ-I))$_2$][PF$_6$]$_2$, 5 by zinc. An excess of zinc powder (20 mg) was added to a red-brown solution of 5 (65.2 mg, 0.05 mmol) in THF (10 ml). The mixture was stirred at room temperature for 10 h, affording a green solution. The solution was filtered and the solvent was removed giving, as above, a green residue. Complexes 6 and 7 were extracted from this residue as described above and were obtained in similar yields.

2.2.5. [{η^5:η^1-C$_5$H$_4$(CH$_2$)$_2$PPh$_2$}RhI)$_2$], 7: reduction of [{(η^5:η^1-C$_5$H$_4$(CH$_2$)$_2$PPh$_2$}Rh(THF)}][PF$_6$], 6, by lithium triethylhydroborate

One equivalent of LiBHEt$_3$ (100 ml of a 1.0 M solution in THF) was added to a green solution of compound 6 (72.4 mg; 0.1 mmol) in THF at -78°C and then stirred at room temperature. After 12 h, the solvent was removed under vacuum to give a green solid from which a single compound was extracted by acetone and clearly identified to be compound 7 by ^{31}P NMR.

2.2.6. [{(η^5:η^1-C$_5$H$_4$(CH$_2$)$_2$PPh$_2$}RhI)$_2$(μ-H)]-[BF$_4$], 8

One equivalent of tetrafluoroboric acid (7 ml of HBF$_4$-O(C$_2$H$_5$)$_2$, 85%) was added to a solution of compound 7 (50.7 mg; 0.05 mmol) in toluene (10 ml) at -78°C and then stirred at room temperature. Progressively a violet precipitate appeared. After 2 h of stirring,

the precipitate was collected, washed with diethyl ether (2 × 2 ml) and dried under vacuum (49.6 mg; 0.045 mmol; 90%). Anal. Calcd. for C$_{38}$H$_{37}$BF$_4$I$_2$P$_2$Rh$_2$: C, 41.41; H, 3.38. Found: C, 41.06; H, 3.62.

2.2.7. Reaction of [{η^5:η^1-C$_5$H$_4$(CH$_2$)$_2$PPh$_2$}M(CF$_3$-COO)$_2$], 3 M = Rh, 4 M = Ir, with lithium triethylhydroborate: formation of [{η^5:η^1-C$_5$H$_4$(CH$_2$)$_2$PPh$_2$}-M(C$_2$H$_4$)], 9 M = Rh, 10 M = Ir

To a solution of complex 3 (60.6 mg; 0.1 mmol) in THF (10 ml) was added dropwise at -78°C two equivalents of LiBHEt$_3$ (0.2 ml of a 1.0 M solution in THF). The solution turned immediately red-orange. The temperature was raised to room temperature and the solvent was removed under vacuum to give a yellow crude material which was soluble in common organic solvents. ^{31}P{1H} NMR spectrum of this material in C$_6$D$_6$ indicated the presence of only one new compound characterized by a doublet centered at 69.39 ppm with a doublet spacing of 213.6 Hz. Compound 9 was then obtained in pure form as orange-yellow crystals upon cooling to -20°C a pentane solution of the crude material (20.4 mg; 50%). Anal. Calcd. for C$_{21}$H$_{22}$PRh: C, 61.78; H, 5.43. Found: C, 61.62; H, 5.50.

Using similar experimental conditions, the treatment of 2 with LiBHEt$_3$ afforded the analogous ethylene derivative 10, as shown by ^{31}P{1H} NMR. Yellow crystals of 10 were obtained from a diethyl ether solution. Anal. Calcd. for C$_{21}$H$_{22}$PIr: C, 50.69; H, 4.46. Found: C, 52.02; H, 4.59.

2.3. Electrochemical studies

Electrochemical measurements were carried out with a home-made potentiostat using interfacing hardware with a PC compatible microcomputer. Positive feedback (scan rate greater than 1 V s^{-1}) or the interrupt method

(scan rate less than 1 V s^{-1}) was used to compensate for *IR* drop. Electrochemical experiments were performed in an airtight three-electrode cell connected to a vacuum/argon line. The cell was degassed and filled according to standard vacuum techniques. The reference electrode consisted of an SCE separated from the solution by a bridge compartment filled with the same solvent and supporting electrolyte solution as used in the cell. The counter electrode was a Pt wire spiral of ca. 8 cm length and 0.5 mm diameter. The working electrode was a 100 mm diameter Pt disk, and the rotating disk electrode (RDE) was a 2 mm diameter Pt disk (Tacussel EDI). With the above reference and bridge system, $E° = 0.54$ V was obtained for 2 mM ferrocene solutions.

2.4. X-ray crystallography

Crystal data for [{η^5:η^1-C$_5$H$_4$(CH$_2$)$_2$PPh$_2$}Rh(CF$_3$COO)$_2$], **3**, and [{{η^5:η^1-C$_5$H$_4$(CH$_2$)$_2$PPh$_2$}Rh(μ-Ì)}$_2$][PF$_6$] · 2OCMe$_2$, **5'**, are summarized in Table 2.

2.5. Structure determination

Reflection data were measured at 20 °C with an Enraf–Nonius CAD-4 diffractometer in the ω–2θ scan

Table 2
Crystal data for [{η^5:η^1-C$_5$H$_4$(CH$_2$)$_2$PPh$_2$}Rh(CF$_3$COO)$_2$], **3** and [{{η^5:η^1-C$_5$H$_4$(CH$_2$)$_2$PPh$_2$}Rh(μ-I)}$_2$][PF$_6$]$_2$ · 2OCMe$_2$, **5'**

	3	5'
Formula	C$_{22}$H$_{18}$F$_6$O$_4$PRh	C$_{44}$H$_{48}$F$_{12}$I$_2$O$_2$P$_4$Rh$_2$
Fw	606.26	1420.4
Crystal system	triclinic	monoclinic
Space group	P1̄ (no. 2)	P2$_1$/c (no. 14)
a (Å)	8.3060(7)	13.838(1)
b (Å)	18.289(2)	13.403(1)
c, Å	7.9724(8)	14.362(1)
α (deg)	94.178(8)	
β (deg)	106.477(8)	104.73(1)
γ (deg)	93.964(7)	
V (Å^3)	1153.2(2)	2576.2(5)
Z	2	2
F(000)	604	1384
D$_c$ (g cm^{-3})	1.747	1.831
λ (Å)	0.71073	0.71073
μ(MoKα) (cm^{-1})	8.71	19.7
Transmiss. coeff. (min–max)	0.834–0.999	0.934–0.999
2θmax (deg)	50	46
No. of reflns. measd.	4067. all unique	3574. all unique
Observn. criterion	$F_o^2 > 3\sigma(F_o^2)$	$F_o^2 > 2\sigma(F_o^2)$
No. of obsd. rflns.	3361	2246
R(F$_o$) [a]	0.041	0.034
Rw [b]	0.042	0.040

[a] $R = \Sigma ||F_o| - |F_c||/\Sigma|F_o|$.
[b] $Rw = [\Sigma w(|F_o| - |F_c|)^2/\Sigma w|F_o|^2]^{1/2}$.

Table 3
Fractional atomic coordinates and isotropic or equivalent isotropic temperature factors (Å^2 × 100) for **3**

Atom	x	y	z	U_{eq}/U_{iso} [a]
Rh	0.62277(5)	0.21076(2)	0.55796(5)	3.60(2)
P	0.3984(2)	0.26554(7)	0.3996(2)	3.82(7)
O(1)	0.6732(4)	0.2913(2)	0.7730(4)	4.4(2)
O(2)	0.7197(6)	0.3850(2)	0.6193(5)	6.4(3)
O(3)	0.4674(5)	0.1622(2)	0.6956(5)	5.4(2)
O(4)	0.5467(6)	0.0503(2)	0.7054(8)	10.0(4)
F(1)	0.7843(7)	0.4771(2)	0.9039(6)	11.2(4)
F(2)	0.6243(7)	0.4088(3)	0.9860(7)	12.9(4)
F(3)	0.8689(8)	0.3922(3)	1.0423(7)	13.3(5)
F(4)	0.2374(5)	0.1314(2)	0.8442(6)	8.6(3)
F(5)	0.1902(6)	0.0370(3)	0.6699(7)	11.4(4)
F(6)	0.3503(6)	0.0361(3)	0.9251(7)	13.5(4)
C(1)	0.4819(7)	0.3023(3)	0.2315(7)	5.5(3)
C(2)	0.5674(7)	0.2400(4)	0.1634(7)	5.8(4)
C(3)	0.6789(7)	0.2049(3)	0.3151(7)	5.0(3)
C(4)	0.8198(7)	0.2410(3)	0.4473(7)	5.1(3)
C(5)	0.8864(7)	0.1888(4)	0.5668(8)	6.2(4)
C(6)	0.7880(8)	0.1233(3)	0.5172(8)	6.1(4)
C(7)	0.6556(7)	0.1319(3)	0.3626(8)	5.4(3)
C(8)	0.7120(6)	0.3576(3)	0.7533(7)	4.5(3)
C(9)	0.7464(9)	0.4095(3)	0.9174(9)	6.4(4)
C(10)	0.4620(5)	0.1025(3)	0.7292(5)	2.6(2)
C(11)	0.3125(8)	0.0760(3)	0.7947(8)	5.4(3)
C(12)	0.2151(4)	0.2037(1)	0.2756(5)	4.3(1) *
C(13)	0.0831(4)	0.2336(1)	0.1590(5)	5.1(1) *
C(14)	−0.0569(4)	0.1879(1)	0.0564(5)	5.4(1) *
C(15)	−0.0648(4)	0.1123(1)	0.0705(5)	5.8(2) *
C(16)	0.0672(4)	0.0823(1)	0.1872(5)	5.8(1) *
C(17)	0.2071(4)	0.1280(1)	0.2897(5)	4.8(1) *
C(18)	0.3136(5)	0.3363(2)	0.5080(4)	4.1(1) *
C(19)	0.2615(5)	0.3182(2)	0.6527(4)	5.0(1) *
C(20)	0.1867(5)	0.3695(2)	0.7372(4)	5.8(2) *
C(21)	0.1639(5)	0.4389(2)	0.6771(4)	6.0(2) *
C(22)	0.2160(5)	0.4570(2)	0.5324(4)	6.7(2) *
C(23)	0.2908(5)	0.4057(2)	0.4479(4)	5.7(1) *

[a] U_{eq} is equal to 1/3 of the orthogonalized U_{ij} tensor. Asterisks denote isotropic U values.

mode using graphite-monochromatized Mo Kα radiation ($\lambda = 0.71073$ Å). A least squares fit of 25 reflections was used to obtain the final lattice parameters and the orientation matrix. Data were reduced in the usual way with the MolEN package [27]. There was no significant variation of standards for **3** and a slight linear decay (7.0%) for **5'**, of which data were corrected [27]. An empirical absorption correction [28] was applied on the basis of ψ scans. The structures were determined by direct methods, using the SHELXS-86 program [29]. Refinements were carried out with the SHELX-76 program [30] using full-matrix least squares techniques minimizing the function $\Sigma w(||F_o| - |F_c||)^2$. Atomic scattering factors (f', f'') were taken from the literature [31].

2.5.1. [{η^5:η^1-C$_5$H$_4$(CH$_2$)$_2$PPh$_2$}Rh(CF$_3$COO)$_2$], 3

Orange plates were obtained at room temperature by slow diffusion of pentane into a dichloromethane solu-
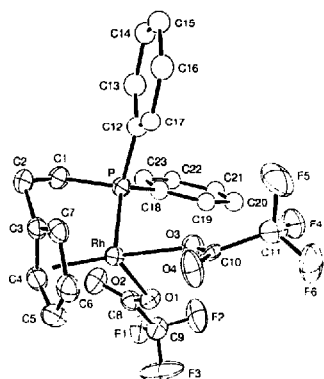
Fig. 1. Perspective representation of the bis(trifluoroacetato) complex 3.

tion of **3**. Phenyl rings were refined as isotropic rigid groups (C–C = 1.395 Å). All other non-H atoms were refined anisotropically. All H atoms were introduced in calculations in idealized geometry (C–H = 0.97 Å) with temperature factors kept fixed to 0.06 Å^2. The refinement converged to $R = 0.041$ and $Rw = 0.042$ with a maximum shift/esd of 0.011 (U_{11} of F(1) atom) on the final cycle with 3361 observations and 232 variable parameters. A fit of $S = 1.26$ was obtained with unit weights. The maximum residual peak was 0.55 e Å^{-3} near an F atom. Table 3 lists the atomic positions for the non-hydrogen atoms. An ORTEP plot [32] of **3** is shown in Fig. 1.

2.5.2. *[{{η^5:η^1-C$_5$H$_4$(CH$_2$)$_2$PPh$_2$}Rh(μ-I)}$_2$]{PF$_6$]$_2$ · 2OCMe$_2$, 5'*

Orange-red parallelepipeds were obtained at room temperature by slow evaporation from a saturated acetone–pentane (1/4) solution of **5**. Phenyl rings were refined as isotropic rigid groups (C–C = 1.395 Å). All other non-H atoms were refined anisotropically, including the found solvent molecule (i.e. acetone) atoms. All H atoms were introduced in idealized geometry (C–H = 0.97 Å) with general isotropic temperature factors kept fixed to 0.07 Å^2 for phenyl H atoms, to 0.13 Å^2 for solvent methyl H atoms and to 0.06 Å^2 for the other H atoms. The refinement converged to $R = 0.034$ and $Rw = 0.040$ with a maximum shift/esd of 0.111 (U_{22} of C(2s) atom) on the final cycle with 2246 observations and 217 variable parameters. A fit of $S = 1.172$ for the data using the weighting scheme $w = [\delta^2(F_o) + 0.0009F_o^2]^{-1}$ was obtained. The maximum residual peak was 0.62 e Å^{-3} on an F atom. Table 4 gives the atomic positions for the non-hydrogen atoms. An ORTEP plot [32] of **5'** is shown in Fig. 2.

Table 4
Fractional atomic coordinates and isotropic or equivalent isotropic temperature factors (Å^2 × 100) for **5'**

Atom	x	y	z	U_{eq} / U_{iso} [a]
I	0.45753(3)	0.40595(3)	0.57426(3)	4.54(3)
Rh	0.46646(3)	0.41041(3)	0.38910(3)	3.69(3)
P(1)	0.3064(1)	0.4614(1)	0.3242(1)	4.09(9)
C(1)	0.2986(5)	0.4482(5)	0.1959(4)	5.0(4)
C(2)	0.3423(5)	0.3472(5)	0.1856(4)	5.6(4)
C(3)	0.4342(4)	0.3220(4)	0.2599(4)	3.7(3)
C(4)	0.4570(5)	0.2545(5)	0.3389(4)	5.0(4)
C(5)	0.5563(4)	0.2696(4)	0.3914(4)	4.6(4)
C(6)	0.5973(5)	0.3475(5)	0.3452(4)	4.8(4)
C(7)	0.5203(4)	0.3802(4)	0.2637(4)	3.4(3)
C(8)	0.2079(3)	0.3828(3)	0.3430(3)	4.3(1) [*]
C(9)	0.1101(3)	0.4018(3)	0.2903(3)	5.7(2) [*]
C(10)	0.0321(3)	0.3415(3)	0.3026(3)	6.0(2) [*]
C(11)	0.0519(3)	0.2622(3)	0.3676(3)	5.0(2) [*]
C(12)	0.1496(3)	0.2431(3)	0.4203(3)	5.6(2) [*]
C(13)	0.2276(3)	0.3034(3)	0.4080(3)	5.0(2) [*]
C(14)	0.2642(3)	0.5855(2)	0.3443(3)	4.5(1) [*]
C(15)	0.2260(3)	0.6031(2)	0.4238(3)	4.9(2) [*]
C(16)	0.1994(3)	0.6997(2)	0.4437(3)	5.1(2) [*]
C(17)	0.2109(3)	0.7786(2)	0.3841(3)	5.5(2) [*]
C(18)	0.2491(3)	0.7610(2)	0.3046(3)	5.2(2) [*]
C(19)	0.2757(3)	0.6644(2)	0.2847(3)	5.3(2) [*]
P(2)	0	0.5	0	5.4(2)
F(1)	0.0473(5)	0.4039(4)	0.0503(4)	10.8(4)
F(2)	0.0778(5)	0.5632(5)	0.0708(4)	12.0(5)
F(3)	0.0689(4)	0.4955(5)	−0.0692(4)	12.4(5)
P(3)	0.5	0.5	0	5.8(2)
F(4)	0.4754(5)	0.5400(5)	0.0927(4)	11.9(4)
F(5)	0.4539(6)	0.3977(5)	0.0147(5)	14.6(6)
F(6)	0.6016(5)	0.4626(6)	0.0613(5)	15.7(6)
O	0.8245(5)	0.4656(6)	0.3808(5)	10.1(5)
C(1s)	0.8456(7)	0.5397(8)	0.3410(7)	8.8(7)
C(2s)	0.9403(9)	0.5995(9)	0.3885(9)	14(1)
C(3s)	0.7883(9)	0.5667(9)	0.2386(8)	13(1)

[a] U_{eq} is equal to 1/3 of the orthogonalized U_{ij} tensor. Asterisks denote isotropic U values.
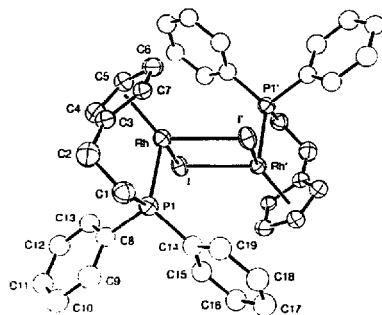

Fig. 2. Perspective representation of the cationic part of the bis(trifluoroacetato) complex **5'**.

3. Results and discussion

The addition of two equivalents of silver trifluoroacetate to the diiodo species $[\{\eta^5:\eta^1\text{-}C_5H_4(CH_2)_2PPh_2\}RhI_2]$, **1**, or $[\{\eta^5:\eta^1\text{-}C_5H_4(CH_2)_2PPh_2\}IrI_2]$, **2**, readily and quantitatively yields quite stable neutral disubstituted monometal products $[\{\eta^5:\eta^1\text{-}C_5H_4(CH_2)_2PPh_2\}Rh(CF_3COO)_2]$, **3**, or $[\{\eta^5:\eta^1\text{-}C_5H_4(CH_2)_2PPh_2\}Ir(CF_3COO)_2]$, **4**. In these compounds, as established by NMR and X-ray experiments (vide infra), the trifluoroacetate anions act as monodentate ligands (Scheme 1).

In these reactions, the substitution of both iodide ligands is observed even when small amounts of the silver salt (less than the 2/1 stoichiometry) were added to **1** or **2**. Typically, a solution containing equivalent amounts of **1** and silver trifluoroacetate exhibits three signals on the $^{31}P\{^1H\}$ NMR spectrum (in C_6D_6-CH_2Cl_2): two doublets of equal intensity at 54.58 ppm ($^1J_{P-Rh} = 146.7$ Hz) and 66.57 ppm ($^1J_{P-Rh} = 149.7$ Hz) for the starting material **1** and the disubstituted product **4** respectively and a third doublet at 62.47 ppm ($^1J_{P-Rh} = 148.0$ Hz) attributed to a monosubstituted intermediate. These three signals are in the intensity ratios 40/40/20 respectively. The addition of growing quantities of silver trifluoroacetate on the mixture is accompanied by a decreasing of the signals corresponding to **1** and to the monosubstituted intermediate and by a concomitant increasing of the signal corresponding to **4**. For the ratio $[1]/[CF_3COO] = 1/1.5$, the signal intensity ratios become 19/23/63, whereas for a ratio of $1/2$, the NMR spectrum indicates only the presence of the disubstituted product **4**.

These observations are consistent with a two-step substitution process in which the first iodide substitution corresponds to a slow rate-determining process followed by a facile second iodide substitution. This indicates a noticeable labilizing effect of the trifluoroacetate group on the remaining iodide ligand.

In contrast with this, the addition of one equivalent of silver hexafluorophosphate to **1** yields readily and
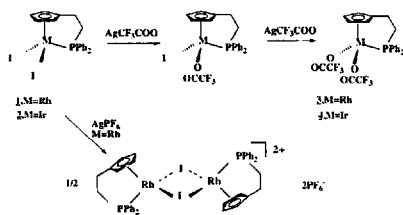
Scheme 1.

Table 5
Selected bond lengths (Å) and angles (deg) with esds in parentheses for **3**

Rh–O(1)	2.103(3)	Rh–P	2.275(1)
Rh–O(3)	2.108(4)	Rh–Cp	1.808(7)
C(1)–C(2)	1.530(9)	C(2)–C(3)	1.514(8)
C(3)–C(4)	1.417(7)	Rh–C(3)	2.114(6)
C(4)–C(5)	1.424(9)	Rh–C(4)	2.127(6)
C(5)–C(6)	1.369(8)	Rh–C(5)	2.236(7)
C(6)–C(7)	1.427(8)	Rh–C(6)	2.243(7)
C(7)–C(3)	1.430(8)	Rh–C(7)	2.133(6)
P–C(1)	1.823(7)		
P–C(12)	1.822(3)	P–C(18)	1.797(4)
P–Rh–O(1)	92.91(9)	P–Rh–Cp	116.8(2)
P–Rh–O(3)	89.3(1)	O(1)–Rh–Cp	128.6(2)
O(1)–Rh–O(3)	81.2(1)	O(3)–Rh–Cp	135.5(2)
C(1)–C(2)–C(3)	110.5(5)	P–C(1)–C(2)	105.9(4)
C(7)–C(3)–C(4)	106.5(5)	C(3)–C(4)–C(5)	107.9(5)
C(4)–C(5)–C(6)	109.3(5)	C(5)–C(6)–C(7)	108.0(5)
C(6)–C(7)–C(3)	108.2(5)		
C(2)–C(3)–C(7)	127.4(4)	C(2)–C(3)–C(4)	125.9(5)
Rh–P–C(1)	101.3(2)	C(1)–P–C(12)	104.2(2)
Rh–P–C(12)	115.9(1)	C(1)–P–C(18)	116.7(2)
Rh–P–C(18)	119.2(1)	C(12)–P–C(18)	104.6(2)

Cp is the centroid of the C(3)C(4)C(5)C(6)C(7) ring.

quantitatively a product clearly identified as a dimetal dicationic species $[\{\{\eta^5:\eta^1\text{-}C_5H_4(CH_2)_2PPh_2\}Rh(\mu\text{-}I)\}_2][PF_6]_2$, **5**.

3.1. Molecular structures of the monometallic [{η⁵:η¹-C₅H₄(CH₂)₂PPh₂}Rh (CF₃COO)₂], 3, and of the dinuclear [{{η⁵:η¹-C₅H₄(CH₂)₂PPh₂}Rh(μ-I)}₂][PF₆]₂, 5, complexes

The molecular structure of **3** is depicted in Fig. 1 and selected bond distances and angles are given in Table 5. This monomeric structure is very similar to that observed for the diiodo complex **1** [26]. The intramolecular coordination of the diphenylphosphino group to the rhodium atom amounts to the formation of a six-membered metallacyclic fragment. Similar geometries has been shown by the X-ray investigations of [(dialkylphosphino)cyclopentadienyl]ruthenium [10] and [(dialkylphosphino)-2,3,4,5-tetramethylcyclopentadienyl]cobalt [11] derivatives as well as by [(dialkylamino)cyclopentadienyl]manganese [14] and molybdenum [15,16] and the [(dialkylamino)-2,3,4,5-tetramethylcyclopentadienyl]cobalt [18], rhodium and iridium [19] derivatives.

The two carboxylate groups are clearly monodentate with the non-bonded oxygen atoms lying approximately 3.2 Å from the metal, (Rh–O(2) = 3.199(4) Å and Rh–O(4) = 3.256(5) Å).

The overall geometry of the metallacyclic fragment may be discussed in terms of the (Rh,P,Cp) plane, (where Cp is the centroid of the cyclopentadienyl ring), the mean plane of the carbon atoms of the cyclopentadienyl ring, and the Rh–Cp and Rh–P vectors.

The differences in the Rh–P distances between the trivalent complexes **1** and **3**, as shown in Table 6, reflect the difference of electron donor abilities of the iodide and the trifluoroacetate ligands, the shortest Rh–P distance being observed in the case of the hardest anionic ligand. Moreover, the Rh–Cp distance in **3** is particularly short and underlines again the great affinity of the cyclopentadienyl group for the hardest acidic center in these types of compound.

As generally observed, the cyclopentadienyl ring is slightly distorted from the corresponding least-square plane (C(3),C(4),C(5),C(6),C(7)), the maximum distance between the carbon atoms and the mean plane being of 0.018(6) Å. The rhodium atom is not centered exactly below the cyclopentadienyl ring, but slightly shifted towards C(3) so that the distances from the rhodium atom to C(3), C(4) and C(7) are shorter than the distances to the other two carbon atoms of the cyclopentadienyl.

The dihedral angle between the mean plane of the carbon atoms of the cyclopentadienyl ring and the (Rh,P,Cp) plane is 90.4(2)°. As already noticed in similar cases [10,11,18,19,26], the C(3)–C(2)–C(1)–P side chain deviates from planarity (torsion angle of −47.0(5)°), the carbon atoms of the ethene bridge C(1) and C(2) being out of the (Rh,P,Cp) plane, on the same side, whereas both phenyl rings attached to the phosphorus are disposed on each side of this plane, as shown in Fig. 3. From these observations, complex **3** is expected to be chiral and the two enantiomers are effectively present in the centrosymmetrical unit cell.

The equivalence of cyclopentadienyl protons, which appear on the ^{1}H NMR spectrum as two ill-resolved multiplets, and the equivalence of protons of each methylene group, which appear as a doublet of triplets (Table 7), even at low temperature, contrast with the crystal structure described above and indicate a very fast fluxional process on the NMR time scale. This process can be described as an oscillation of the Ph$_2$P fragment around the Rh–P axis with inversion of the Rh–P–CH$_2$–CH$_2$–C$_5$H$_4$ ring, and oscillation of the cyclopentadienyl ring around the Rh–Cp axis.

Complex **5** was recrystallized from pentane–acetone. This leads to crystals of **5′** containing complex **5** together with acetone in a 1/2 ratio. The cationic part of **5′** is shown in Fig. 2 and selected bond distances and
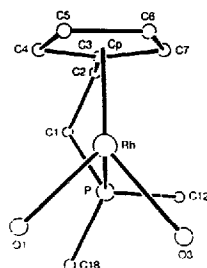

Fig. 3. View of complex **3** along the (Cp,Rh,P) plane showing the deviation from planarity of the P–C(1)–C(2)–C(3) side chain.

angles are given in Table 8. It consists of a centrosymmetrical dinuclear structure containing two rhodium atoms bridged by two iodides, each metal atom being chelated by a (cyclopentadienylethyl)diphenylphosphine. An intermetal separation of 3.9080(8) Å precludes a normal metal–metal bond.

The centrosymmetrical properties demand the coplanarity of Rh, Rh′, I and I′ atoms. The dihedral angle between (Rh,Rh′,I,I′) and (Rh,P(1),Cp) planes and between (Rh,P(1),Cp) and the mean plane of the carbon atoms of the cyclopentadienyl ring are 90.73(7)° and 88.3(2)° respectively.

As in the case of complex **3**, the C(3)–C(2)–C(1)–P(1) side chain in **5′** deviates from planarity, with a torsion angle of −42.8(7)°, and a similar fluxional process in solution, including oscillation of the PPh$_2$ fragment around the Rh–P axis and inversion of the Rh–P–CH$_2$–CH$_2$–C$_5$H$_4$ ring, is again required to explain the apparent symmetry revealed by the ^{1}H NMR data (Table 7).

3.2. Reactions of the trivalent monometallic complexes 1–4 towards hydroborates: formation of ethylene complexes

In order to investigate further the chemical potentialities of the metallacyclic fragment, $[(C_5H_4)(CH_2)_2PPh_2M^{III}]$, we planned to synthesize polyhydride derivatives starting from the trivalent metal

Table 6
Comparable RhCp and RhP distances and PRhCp angles in selected chelate complexes

	RhCp (Å)	RhP (Å)	PRhCp (deg)
$[(\eta^5:\eta^1-C_5H_4(CH_2)_2PPh_2)Rh(C_2H_4)]$, **9** [a]	1.896(6)	2.189(1)	118.5(2)
$[(\eta^5:\eta^1-C_5H_4(CH_2)_2PPh_2)RhI_2]$, **1** [a]	1.844(8)	2.267(2)	117.3(3)
$[(\eta^5:\eta^1-C_5H_4(CH_2)_2PPh_2)Rh(CF_3COO)_2]$, **3**	1.808(7)	2.275(1)	116.8(2)
$[((\eta^5:\eta^1-C_5H_4(CH_2)_2PPh_2)Rh(\mu-I))_2][PF6]_2 \cdot 2OCMe_2$ **5′**	1.837(6)	2.278(2)	115.2(2)

[a] From Ref. [26].

species **1–4** by treatment with hydroborate salts. Different behaviors were observed, depending on the hydroborates and on the complexes **1–4**.

It was first observed that the bis(trifluoroacetato) iridium complex **4** in THF reacts with two equivalents of sodium tetrahydroborate to yield a non-isolated hydrido derivative. This thermally sensitive product was only characterized by ^{1}H NMR which revealed: in the high field region, a triplet centered at -8.89 ppm with a $^2J_{H-P}$ coupling constant of 13.3 Hz; in the cyclopentadienyl region, four multiplets of equal intensity centered at 5.52, 5.12, 5.02 and 4.75 ppm; in the methylene region, four multiplets at 2.90, 2.65, 1.85 and 1.70 ppm. These data are consistent with a dinuclear structure in which two equivalent bridging hydrides would be coupled to two equivalent phosphorus nuclei. According to that and in agreement with the stoichiometric conditions, the tetrahydroborate would act as a reducing and

as a hydriding agent to yield the hypothetical diiridium(II) compound $[\{(\eta^5:\eta^1\text{-}C_5H_4(CH_2)_2PPh_2)Ir(\mu\text{-}H)\}_2]$.

It was also observed that the diiodo rhodium complex **1** reacts with two equivalents of LiBHEt$_3$ to yield a non-isolated thermally sensitive hydride derivative. The ^{31}P{^{1}H} NMR spectrum of this compound exhibits a doublet at 48.36 ppm ($^1J_{P-Rh} = 162.7$ Hz). The ^{1}H NMR spectrum exhibits: in the high-field region, a 1:4:6:4:1 quintet centered at -16.43 ppm which may be analyzed, in a first-order approximation, as an accidentally degenerated triplet of triplets due to hydride protons coupled to two equivalent rhodium nuclei and to two equivalent phosphorus nuclei and with $^1J_{H-Rh} = {}^2J_{H-P} = 24.6$ Hz; in the cyclopentadienyl region, four multiplets centered at 5.85, 5.33, 4.72 and 4.52 ppm; in the methylene region, complexed multi-line patterns in the range 1.5–3 ppm due to non-equivalent and mutually

Table 7
^{1}H NMR data of the isolated ((cyclopentadienylethyl)diphenylphosphine) rhodium and iridium complexes

	δH(Cp) (ppm)	δH(CH$_2$) (ppm)	J_{HP} (Hz)	$^3J_{HH}$ (Hz)	Others (δH (ppm), J (Hz))
1 [a]	5.35(m,2H)	2.66(dt,2H)	10.2	6.6	
	4.85(m,2H)	1.17(dt,2H)	32.7		
2 [d]	6.04(m,2H)	3.10(dt,2H)	9.8	6.9	
	5.57(m,2H)	2.11(dt,2H)	28.1		
3 [a]	5.70(m,2H)	2.72(dt,2H)	11.2	7.2	
	5.30(m,2H)	1.31(dt,2H)	34.1		
4 [a]	5.91(m,2H)	2.60(dt,2H)	10.3	7.0	
	5.29(m,2H)	1.62(dt,2H)	29.2		
5 [b]	6.05(m,8H)	3.96(dt,4H)	10.6	7.1	
		2.36(dt,4H)	36.6		
6 [b]	5.95(m,1H)	3.68(m,1H)			
	5.83(m,1H)	2.55(m,1H)			
	5.05(m,1H)	2.04(m,1H)			
	3.19(m,1H)	1.32(m,1H)			
7 [b]	6.11(m,2H)	3.34(m,2H)			
	5.65(m,2H)	2.85(m,2H)			
	5.01(m,2H)	1.87(m,4H)			
	4.44(m,2H)				
8 [c]	6.92(m,2H)	2.97(m,2H)			δH(hydride) $^2J_{HP}$ $^3J_{HRh}$
	6.55(m,2H)	2.64(m,2H)			-12.89(tt,1H) 11.4 22.8
	5.45(m,2H)	2.01(m,2H)			
	5.17(m,2H)	1.64(m,2H)			
9 [a]	5.87(m,2H)	2.87(dt,2H)	9.5	6.8	δH(C$_2$H$_4$)
	5.30(m,2H)	2.04(dt,2H)	30.7		2.40(m,2H)
					1.12(m,2H)
10 [a]	5.53(m,2H)	2.91(dt,2H)	9.5	6.9	2.70(m,2H)
	5.12(m,2H)	1.77(dt,2H)	27.5		1.54(m,2H)

(m) multiplet; (dt) doublet of triplets; (tt) triplet of triplets.
[a] In C$_6$D$_6$.
[b] In acetone-d_6.
[c] In CD$_2$Cl$_2$.
[d] In CDCl$_3$.

Table 8
Selected bond lengths (Å) and angles (deg) with esds in parentheses
for **5**

Rh · · · Rh'	3.9080(8)	I · · · I'	3.6827(9)
Rh–I	2.6940(6)	Rh–P(1)	2.278(2)
Rh–I'	2.6758(6)	Rh–Cp	1.837(6)
C(1)–C(2)	1.505(9)	C(2)–C(3)	1.476(8)
C(3)–C(4)	1.423(8)	Rh–C(3)	2.151(5)
C(4)–C(5)	1.404(8)	Rh–C(4)	2.204(6)
C(5)–C(6)	1.430(9)	Rh–C(5)	2.255(6)
C(6)–C(7)	1.436(7)	Rh–C(6)	2.229(7)
C(7)–C(3)	1.414(8)	Rh–C(7)	2.155(6)
P(1)–C(1)	1.827(6)		
P(1)–C(8)	1.797(4)	P(1)–C(14)	1.810(4)
Rh–I–Rh'	93.40(1)		
I–Rh–I'	86.60(1)	I'–Rh–P(1)	95.58(4)
I–Rh–P(1)	97.28(4)	I'–Rh–Cp	125.0(2)
I–Rh–Cp	129.0(2)	P(1)–Rh–Cp	115.2(2)
C(1)–C(2)–C(3)	115.4(5)	P(1)–C(1)–C(2)	105.3(4)
C(7)–C(3)–C(4)	107.8(4)	C(3)–C(4)–C(5)	109.0(5)
C(4)–C(5)–C(6)	107.8(5)	C(5)–C(6)–C(7)	107.6(5)
C(6)–C(7)–C(3)	107.8(5)		
C(2)–C(3)–C(7)	117.7(5)	C(2)–C(3)–C(4)	134.3(6)
Rh–P(1)–C(1)	100.7(2)	C(1)–P(1)–C(8)	104.0(2)
Rh–P(1)–C(8)	117.3(1)	C(1)–P(1)–C(14)	108.1(2)
Rh–P(1)–C(14)	122.0(1)	C(8)–P(1)–C(14)	103.1(2)

i is the symmetry operation $1 - x$, $1 - y$, $1 - z$. Cp is the centroid of the C(3)C(4)C(5)C(6)C(7) ring.

coupled protons. As above, these data suggest a dirhodium(II) structure containing bridging hydride ligands.

Contrasting with this behavior, the treatment of the bis(trifluoroacetato) complexes **3** and **4** with two equivalents of lithium triethylhydroborate under similar experimental conditions leads to the reduction products **9** and **10** respectively. As indicated by a $J_{P–Rh}$ value of 213.6 Hz (Table 1), the product **9** was expected to be a rhodium(I) species. Then, it was unambiguously identified as the already known ethylene complex $[(\eta^5:\eta^1\text{-}C_5H_4(CH_2)_2PPh_2)Rh(C_2H_4)]$, **9**, (Scheme 2 and Tables 1 and 7) by usual analytical methods and by comparison of its spectroscopic properties with those of an authentic sample [26]. $[(\eta^5:\eta^1\text{-}C_5H_4(CH_2)_2\text{-}PPh_2)Ir(C_2H_4)]$, **10**, was obtained similarly by treatment of **4** with LiBHEt₃ in THF.

In these reactions, the source of ethylene is not yet clearly understood. The literature provides few interesting precedents. The first one concerns the behavior of $[RhI_2(PPh_3)(\eta^5\text{-}C_5Me_5)]$ towards ω-di-Grignard

Scheme 2.
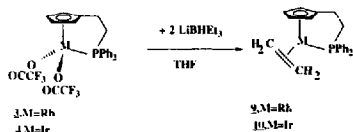
reagents, reported by Diversi et al. [33]. An ethylene–rhodium complex was one of the products obtained when diethyl ether was used as solvent and it was shown by deuterium-labeling experiments that this solvent was the source of ethylene. Thus, it should be considered that the reaction of **3** with LiBHEt₃ in THF follows a similar pathway, i.e. that THF reacts with LiBHEt₃ to yield ethylene. This hypothesis implies that the hydroborate acts as a reductant to reduce both THF into ethylene and rhodium(III) complex **3** into a rhodium(II) complex. This is not inconsistent with the stoichiometric conditions of our experiments, i.e. [LiBHEt₃]/[3] = 2. Nevertheless, if it is known that strong reductants like BuLi are easily able to reduce THF to yield ethylene, to our knowledge this is not the case of LiBHEt₃. A second precedent concerns the observations reported by Thaler and Caulton [34] on the reaction of [RhCl(C₂H₄)(triphos)] with tetraethylborate to yield [RhH(C₂H₄)(triphos)]. In this reaction, labeling experiments demonstrated that the ethylene ligand in the final product was derived from tetraethylborate and not from the ethylene initially present in the starting material. But this involves only Rh(I) complexes, in the starting material, in the ethyl–ethylene intermediate, and in the final product as well whereas, in our case, the final ethylene product is the result of a reductive process.

This behavior of complexes **3** and **4** towards lithium triethylhydroborate draws attention to a specific role of the acetato ligand in the formation of the ethylene complexes and calls for further experiments.

3.3. Reduction of complex 5

A cationic monometal species containing THF, $[(\eta^5:\eta^1\text{-}C_5H_4(CH_2)_2PPh_2)RhI(THF)][PF_6]$, **6**, and a dinuclear neutral species, $[\{\{\eta^5:\eta^1\text{-}C_5H_4(CH_2)_2PPh_2\}RhI\}_2]$, **7**, were obtained in almost 2:1 relative amounts upon treatment of complex **5** with two equivalents of lithium triethylhydroborate, or with an excess of zinc powder.

The asymmetric structure of the complex **6**, due to the presence of two different terminal ligands, was confirmed by the non-equivalence of the four cyclopentadienyl protons and the non-equivalence of the four methylene protons of the ethene bridge, as revealed by the ¹H NMR data (Table 7).

In the absence of crystals suitable for X-ray analysis, the structure of **7** was deduced from analytical and NMR data. From analytical data, compound **7** appears as a rhodium(II) species. This observation, which was confirmed by electrochemistry (vide infra), together with magnetic properties, strongly suggests a dinuclear structure with a metal–metal bond. Electron-counting implies that the iodides necessarily occupy terminal posi-
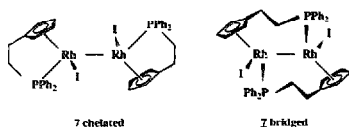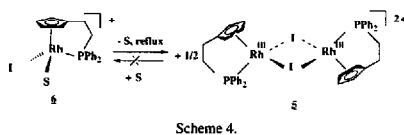
Scheme 3.

Scheme 4.

tions, one on each metal. The symmetrical arrangement of the phosphorus atoms is confirmed by the $^{31}P\{^1H\}$ NMR spectrum which exhibits a single doublet, centered at 38.60 ppm. The ^1H NMR spectrum exhibits non-equivalent cyclopentadienyl protons and non-equivalent methylene protons, consistent with a molecular structure having a two-fold axis or a center of symmetry. Such a molecular structure may accommodate (cyclopentadienylethyl)diphenylphosphine acting either as chelating or bridging ligands. Scheme 3 shows these two possibilities in the hypothesis of a two-fold axis molecular structure. The possibility that the cyclopentadienylphosphine ligands in **7** and in the related protonated compound **8** (vide infra) are bridging can be questioned on the ground of the ^{31}P chemical shifts — a difference of ca. 20 ppm being observed between the complexes known to be chelated and the complexes **7** and **8** (Table 1). This suggestion is also consistent with our previous observations on the chelated $[\{\eta^5:\eta^1-C_5H_4(CH_2)_2PPh_2\}Rh(CO)]$ and on the bridged $[\{(\mu-\eta^5:\eta^1-C_5H_4(CH_2)_2PPh_2\}Rh(CO)]_2]$ complexes [26].

The proposed metal–metal bond of complex **7** must act as a basic site, and this was confirmed by a protonation experiment. The protonation of **7** yields a red salt for which the ^1H NMR spectrum revealed a bridging proton between rhodium atoms. In the high-field region, the ^1H NMR spectrum exhibits a 1:2:3:4:3:2:1 septet which may be analyzed, in a first-order approximation, as an accidentally degenerated triplet of triplets due to a proton coupled to two equivalent rhodium nuclei and to two equivalent phosphorus nuclei ($^1J_{H-Rh} = 2 \times {}^2J_{H-P} = 22.8$ Hz) (Table 7). This indicates that the symmetry of **7** is retained in **8** and suggests that the added proton is located on the element of symmetry. The protonation is a reversible process and the starting material **7** was readily recovered from acetone solution of **8**.

The starting material **5** can be recovered from **6** after elimination of coordinated THF in refluxing toluene solution of **6** (Scheme 4), and complex **6** can be quantitatively reduced to **7** but only after a prolonged treatment with one equivalent of lithium triethylhydroborate (Scheme 5).

A key point concerns the formation of **6**. Formally this complex can be considered as a simple product of solvolysis of **5** by THF. In fact, we checked that it was not possible to get this complex just upon warming THF

solution of **5** and its formation from **5** was clearly the consequence of a reduction process.

For this reason, we undertook an electrochemical study of complex **5** including cyclic voltammetry, coulometry and preparative electrolysis. A typical voltammogram at 0.1 V s^{-1} for the reduction of complex **5** in CH_2Cl_2–Bu_4NBF_4 (1 M) at a Pt-disk electrode is given in supplementary material. The first cathodic scan shows two successive irreversible reduction peaks P_1 and P_2 with cathodic peak potentials E_{P1} and E_{P2} at -0.29 V and -1.11 V respectively.

Bulk electrolysis controlled-potential coulometry experiments carried out at -0.70 V gave a green solution and an n_{app} value (faradays per mole of reactant consumed) of unity. No ESR signal was observed from the resulting green solution, whereas the $^{31}P\{^1H\}$ NMR spectrum in acetone exhibits two doublets of equal intensity at 65.60 and 38.60 ppm, indicating clearly the conversion of the starting material **5** into **6** and **7**. As expected, the voltammogram of the green solution exhibits only one peak at -1.11 V.

The chemical or electrochemical formation of complexes **6** and **7** is therefore the consequence of an
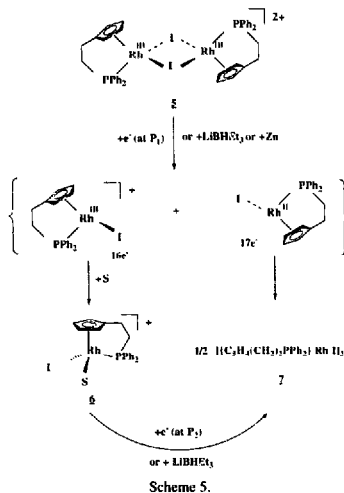
Scheme 5.

irreversible one-electron reduction which corresponds to the reduction peak P_1 of the voltammogram. The addition of a single electron to complex **5** leads to a $37e^-$ derivative which is expected to yield, upon cleavage of the iodo bridges, the hypothetical 16 and $17e^-$ fragments shown on Scheme 5. Complex **6** must result, then, from the coordination of a solvent molecule to the $16e^-$ fragment, whereas **7** must result from the dimerization of the $17e^-$ fragment. As previously mentioned, the solvated rhodium(III) cation **6** is chemically reduced to yield **7**, (vide supra); electrochemically, this reduction is observed at the potential P_2.

4. Supplementary material available

Listings of H atom parameters, anisotropic thermal parameters, all bond distances and angles, and least-square planes and deviations therefrom (10 pages). Voltammogram for the reduction of complex **5** (1 page). Ordering information is given on any current masthead page.

References

[1] (a) D.W. Macomber, W.P. Hart and M.D. Rausch, *Adv. Organomet. Chem.*, *21* (1982) 1. (b) N.J. Coville, K.E. du Plooy and W. Pickl, *Coord. Chem. Rev.* (1992) 1.

[2] (a) W.R. Cullen, T.J. Kim, F.W.B. Einstein and T. Jones, *Organometallics*, *4* (1985) 346. (b) W.R. Cullen, F.W.B. Einstein, C.H. Huang, A.C. Willis and E.S. Yeh, *J. Am. Chem. Soc.*, *102* (1980) 988.

[3] T. Hayashi, M. Konishi, Y. Kobori, M. Kumada, T. Higuchi and K. Hirotsu, *J. Am. Chem. Soc.*, *106* (1984) 158.

[4] J.C. Flores, J.C.W. Chien and M.D. Rausch, *Organometallics*, *13* (1994) 4140.

[5] N.J. Long, *Angew. Chem. Int. Ed. Engl.*, *34* (1995) 21.

[6] F. Mathey and J.P. Lampin, *Tetrahedron*, *31* (1975) 2685.

[7] X.D. He, A. Maisonnat, F. Dahan and R. Poilblanc, *Organometallics*, *6* (1987) 678.

[8] (a) J.K. Stille, C. Smith, O.P. Anderson and M.M. Miler, *Organometallics*, *8* (1989) 1040. (b) M.D. Rausch, W.C. Spink, J.L. Atwood, A.J. Baskar and S.G. Bott, *Organometallics*, *8* (1989) 2627. (c) X.D. He, A. Maisonnat, F. Dahan and R. Poilblanc, *Organometallics*, *8* (1989) 2618. (d) G.K. Anderson, M. Lin and M.Y. Chiang, *Organometallics*, *9* (1990) 288. (e) X.D. He, A. Maisonnat, F. Dahan and R. Poilblanc, *J. Chem. Soc. Chem. Commun.*, (1990) 670. (f) X.D. He, A. Maisonnat,

F. Dahan and R. Poilblanc, *New J. Chem.*, *14* (1990) 313. (g) X.D. He, A. Maisonnat, F. Dahan and R. Poilblanc, *Organometallics*, *10* (1991) 2443. (h) J.B. Tommasino, D. de Montauzon, X.D. He. A. Maisonnat, R. Poilblanc, J.N. Verpeaux and C. Amatore. *Organometallics*, *11* (1992) 4150. (i) B. Brumas, F. Dahan, D. de Montauzon and R. Poilblanc, *J. Organomet. Chem.*, *453* (1993) C13. (j) B. Brumas, D. de Caro, F. Dahan, D. de Montauzon and R. Poilblanc, *Organometallics*, *12* (1993) 1503. (k) B. Brumas-Soula, D. de Montauzon and R. Poilblanc, *New J. Chem.*, *19* (1995) 757. (l) F.T. Ladipo, G.K. Anderson and N.P. Rath, *Organometallics*, *13* (1994) 4741.

[9] (a) J.C. Leblanc, C. Moïse, A. Maisonnat, R. Poilblanc, C. Charrier and F. Mathey, *J. Organomet. Chem.*, *231* (1982) C43. (b) C.P. Casey, R.M. Bullock, W.C. Fultz and A.L. Rheingold, *Organometallics*, *1* (1982) 1591. (c) M.D. Rausch, B.H. Edwards, R.D. Rogers and J.L. Atwood, *J. Am. Chem. Soc.*, *105* (1983) 3882. (d) C.P. Casey, R.M. Bullock and F. Nief, *J. Am. Chem. Soc.*, *105* (1983) 7574. (e) C.P. Casey and R.M. Bullock, *Organometallics*, *3* (1984) 1100. (f) C.P. Casey and F. Nief, *Organometallics*, *4* (1985) 1218. (g) D.L. du Bois, C.W. Eigenbrot, Jr, A. Miedaner, J.C. Smart and R.C. Haltiwanger, *Organometallics*, *5* (1986) 1405. (h) W. Tikkanen, Y. Fujita and J.L. Petersen, *Organometallics*, *5* (1986) 888. (i) R.M. Bullock and C.P. Casey, *Acc. Chem. Res.*, *20* (1987) 167. (j) L.B. Kool, M. Ogasa, M.D. Rausch and R.D. Rogers, *Organometallics*, *8* (1989) 1785. (k) M. Ogasa, M.D. Rausch and R.D. Rogers, *J. Organomet. Chem.*, *403* (1991) 279.

[10] A.M.Z. Slawin, D.J. Williams, J. Crosby, J.A. Ramsden and C. White, *J. Chem. Soc. Dalton Trans.*, (1988) 2491.

[11] H. Butenschön, R.T. Kettenbach and C. Krüger, *Angew. Chem. Int. Ed. Engl.*, *31* (1992) 1066.

[12] R.T. Kettenbach and H. Butenschön, *New J. Chem.*, *14*, (1990) 599.

[13] (a) T. Kauffmann, J. Ennen, H. Lhotak, A. Rensing, F. Steinseifer and A. Woltermann, *Angew. Chem. Int. Ed. Engl.*, *19* (1980) 328. (b) T. Kauffmann and J. Olbrich, *Tetrahedron Lett.*, *25* (1984) 1967.

[14] T.F. Wang, T.Y. Lee, Y.S. Wen and L.K. Liu, *J. Organomet. Chem.*, *403* (1991) 353.

[15] T.F. Wang, T.Y. Lee, J.W. Chou and C.W. Ong, *J. Organomet. Chem.*, *423* (1992) 31.

[16] T.F. Wang and Y.S. Wen, *J. Organomet. Chem.*, *439* (1992) 155.

[17] A. Avey, T.J.R. Weakley and D.R. Tyler, *J. Am. Chem. Soc.*, *115* (1993) 7706.

[18] P. Jutzi, M.O. Kristen, J. Dahlhaus, B. Neumann and H.G. Stammler, *Organometallics*, *12* (1993) 2980.

[19] P. Jutzi, M.O. Kristen, B. Neumann and H.G. Stammler, *Organometallics*, *13* (1994) 3854.

[20] (a) W.A. Herrmann, M.J.A. Morawietz and T. Priermeier, *Angew. Chem. Int. Ed. Engl.*, *33* (1994) 1946. (b) W.A. Herrmann, M.J.A. Morawietz, T. Priermeier and K. Mashima, *J. Organomet. Chem.*, *486* (1995) 291.

[21] J.R. Van den Hende, P.B. Hitchcock, M.F. Lappert and T.A. Nile, *J. Organomet. Chem.*, *472* (1994) 79.

[22] (a) A.K. Hughes, A. Meetsma and J.H. Teuben, *Organometallics*, *12* (1993) 1936. (b) U. Böhme and K.H. Thiele, *J. Organomet. Chem.*, *472* (1994) 39.

[23] D.M. Antonelli, M.L.H. Green and P. Mountford, *J. Organomet. Chem.*, *438* (1992) C4.

[24] (a) H. Qichen, Q. Yanlong, L. Guisheng and T. Youqi, *Transition Met. Chem.*, *15* (1990) 483. (b) R. Fandos, A. Meetsma and J.H. Teuben, *Organometallics*, *10* (1991) 59.

[25] K.H. Zimmermann, R.S. Pilato, I.T. Horvath and J. Okuda, *Organometallics*, *11* (1992) 3935.

[26] I. Lee, F. Dahan, A. Maisonnat and R. Poilblanc, *Organometallics*, *13* (1994) 2743.

[27] C.K.Fair, *MolEN: Structure Solution Procedures*, Enraf–Nonius, Delft, Netherlands, 1990.

[28] A.C.T. North, D.C. Phillips and F.S. Matews, *Acta Cristallogr. Sect. A:, 24* (1968) 351.

[29] G.M. Sheldrick, SHELXS-86, *Program for Crystal Structure Solution*, University of Göttingen, Göttingen, Germany, 1986.

[30] G.M. Sheldrick, SHELX-76, *Program for Crystal Structure Determination*, University of Cambridge, Cambridge, UK. 1976.

[31] *International Tables for X-Ray Crystallography*, Vol. IV, Kynoch Press, Birmingham, UK, 1974, Table 2.2.B, pp. 99–101 and Table 2.3.1., p. 149.

[32] C.K. Johnson, ORTEP, *Rep. ORNL-3794*, 1965 (Oak Ridge National Laboratory, Oak Ridge, TN, USA).

[33] P. Diversi, G. Ingrosso, A. Lucherini, P. Martinelli, M. Benetti and S. Pucci, *J. Organomet. Chem., 165* (1979) 253.

[34] E.G. Thaler and K.G. Caulton, *Organometallics, 9* (1990) 1871.